Error Analysis of the NIST Optically Pumped Primary Frequency Standard

Robert E. Drullinger, Jon H. Shirley, J. P. Lowe, and David J. Glaze

Abstract—**The major sources of systematic error in the NIST optically pumped primary frequency standard have been evaluated with an uncertainty of a few parts in 10^{14}. The cavity end-to-end phase shift is the only item which differed markedly from expectations based on the design and/or measurements made during assembly. We think the difference is attributable to the physical dimensions of the cavity and not to its asymmetry. The device will begin to function as the U.S. primary frequency standard, even before planned extensions to the analysis presented here and improvements to the laser and servo electronics allow evaluation at its full design accuracy of one part in 10^{14}.**

I. Introduction

We report an analysis of the frequency errors in the optically pumped primary frequency standard constructed at NIST [1] and known as NIST-7. The standard will be further developed in stages and will ultimately operate continuously as a primary *clock*. The work presented here will be followed by additional measurements and modifications to the servo system before evaluation at the full design potential of one part in 10^{14}. Development of a servo system that not only controls the clock frequency but also the microwave power and the value of the C-field will be necessary before it is operated as a primary clock.

The standard has a Ramsey cavity 1.55 m long and an atomic beam 3 mm in diameter. An axial C-field geometry is employed and the atomic beam goes through the X-band waveguide cavity parallel to the long dimension of the waveguide. The microwave field, therefore, varies as a half-sine wave in the direction of the atomic beam resulting in Rabi lineshapes with very smooth and rapidly damped tails (see Fig. 1). The cavity ends are designed so the Poynting vector vanishes in the center of the atomic beam window [2], thus minimizing distributed-cavity-phase-shift effects.

For the experiments reported here, a single, grating-feedback diode laser (linewidth ≤ 100 kHz) was frequency-locked to the $F = 4 \rightarrow F' = 3$ saturated-absorption feature in an external cesium cell. Approximately 0.1 mW in a 3 mm diameter ($2w_0$) light beam with linear polarization was used for state preparation. The optical pumping beam was orthogonal to the atomic beam and was retro-reflected on itself with its polarization rotated 90°. This creates a zone of "randomized polarization" which leads to complete optical pumping ($\geq 99.9\%$) and avoids the problem of coherence trapping [3]. An acousto-optic device was used to synthesize a second light beam with the ≈ 450 MHz offset necessary to drive the $F = 4 \rightarrow F' = 5$ cycling transition in the detection region. The power density in this beam was adjusted to scatter approximately 10 photons per atom. The overall fluorescence collection-and-detection efficiency is $\geq 40\%$.

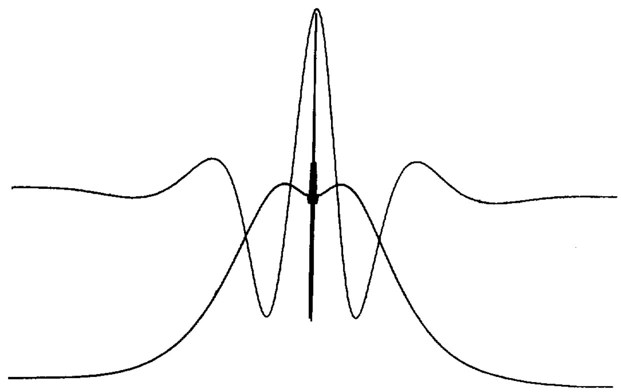

Fig. 1. The Rabi and Ramsey line shapes for the "clock" transition recorded at optimum power. The scan widths are 35 kHz and 1 kHz, respectively. The dip in the center of the Rabi line is a result of the very low velocity atoms that contribute to the signal in an optically pumped standard and is enhanced by the use of a cycling transition for detection.

Measurements of frequency shifts were made relative to an active hydrogen maser. At present, the stability of the standard is characterized by $\sigma_y(\tau) \leq 1 \times 10^{-12}\tau^{-1/2}$ (Fig. 2) and is not limited by atomic shot noise at oven temperatures above 90°C. The frequency biases and their associated uncertainties are quoted throughout this paper in terms of fractional frequency change in the standard.

II. Static Magnetic Field Effects

The correction for second-order Zeeman effect is made by measuring the first-order Zeeman splitting. This measurement can have very high precision, but the *accuracy* of the resulting correction is limited by C-field inhomogeneity and instability. In NIST-7, the field inhomogeneity is relatively small (see Fig. 3). Its dependence on field strength and interchange of shield parts indicates that it originates from the imperfect fit of the end caps on the

Manuscript received June 12, 1992; revised October 21, 1992.

The authors are with the National Institute of Standards and Technology, Boulder, CO 80303.

IEEE Log Number 9206473.

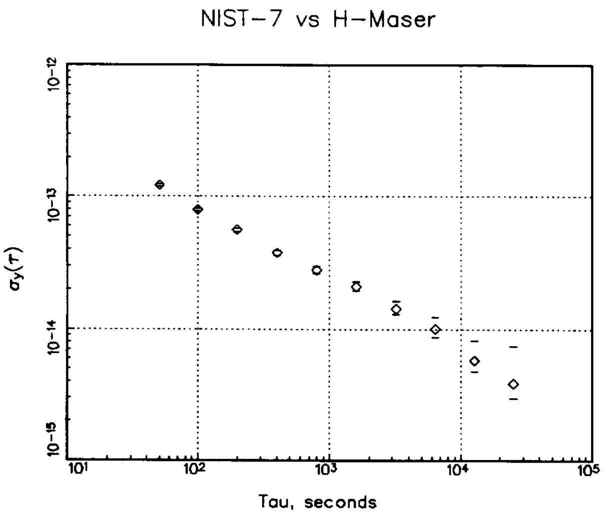

Fig. 2. Frequency stability of NIST-7 measured against an active hydrogen maser. The error bars represent 1σ on the statistics of the measurement.

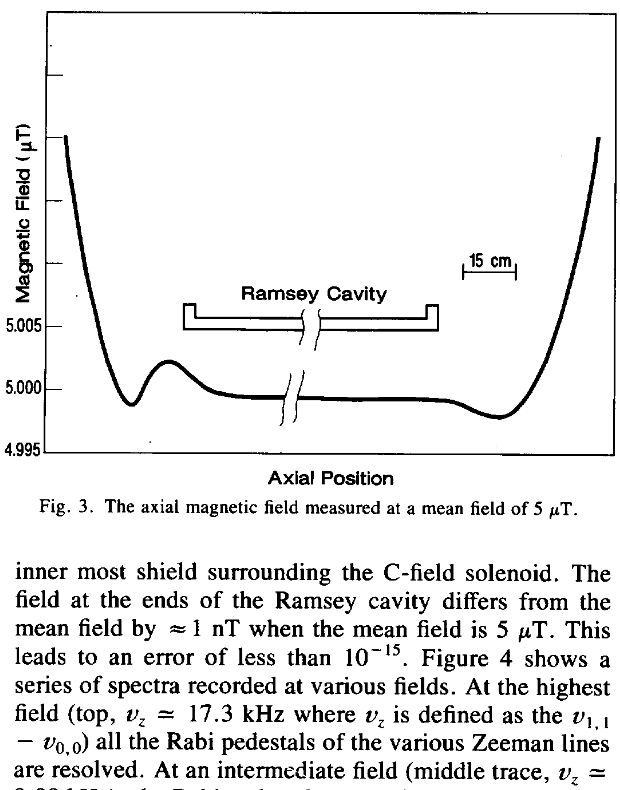

Fig. 3. The axial magnetic field measured at a mean field of 5 μT.

inner most shield surrounding the C-field solenoid. The field at the ends of the Ramsey cavity differs from the mean field by ≈ 1 nT when the mean field is 5 μT. This leads to an error of less than 10^{-15}. Figure 4 shows a series of spectra recorded at various fields. At the highest field (top, $v_z \simeq 17.3$ kHz where v_z is defined as the $v_{1,1} - v_{0,0}$) all the Rabi pedestals of the various Zeeman lines are resolved. At an intermediate field (middle trace, $v_z \simeq 0.99$ kHz), the Rabi pedestals are no longer resolved, but the seven Ramsey resonances can be seen. At the lowest field (bottom trace, C-field current off), all the Ramsey resonances coalesce into a single peak only 10% wider than one of the single, resolved Ramsey resonances. This indicates a residual field of less than 2 nT, which is in agreement with measurements made on the field during assembly.

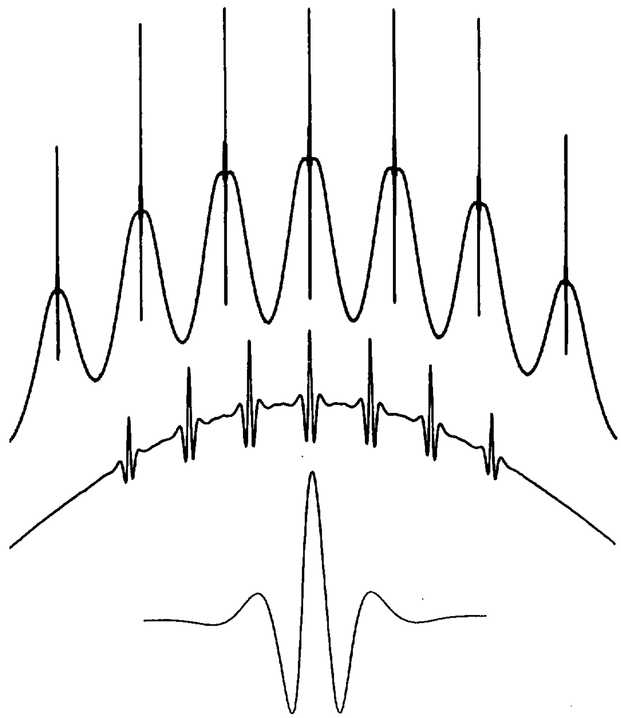

Fig. 4. The entire Zeeman spectrum recorded at three different magnetic fields. At the highest field (top, $v_z \simeq 17.3$ kHz) the Rabi lines are resolved. At an intermediate field (middle trace, $v_z \simeq 0.99$ kHz) the Rabi lines are no longer resolved but the seven Ramsey lines remain so. At "zero" field in the lowest trace, the C-field driving current has been set to zero. The Ramsey lines coalesce into a single line only 10% wider than one of the single, resolved Ramsey resonances in the traces above. The scales change from trace to trace.

Instability in the C-field can result from fluctuations of the current source, the physical size of the coil form, or leakage of external fields through the shields. The stability of the current source as well as thermal and mechanical stability of the coil form lead to errors of less than 10^{-15}. The magnetic shield package in NIST-7 consists of three concentric shields made of high μ material 1.5 mm thick. Each shield has a degaussing coil wound toroidally on the cylindrical wall. The axial shielding factor results in a sensitivity to external, axial fields of about $2 \times 10^{-14}/\mu$T for the purely passive shield package when operated at a field value of 4 μT. We have shown that magnetic "shaking," in effect a continuous, low level degaussing of the outer two shields, improves the axial shielding factor by an order of magnitude and appears to lead to no frequency offsets or degradation of clock operation.

III. Second-Order Doppler Shift

In the present analysis, correction for the second-order Doppler shift was made by numerical evaluation of a formula that accounts for the atomic velocity distribution, the microwave power and the characteristics of the modulation [4]. The velocity distribution used was the theoretical one for a thermal beam weighted by $1/v$ for detection by a cycling transition:

$$f(v) = 4\pi^{-1/2} v^2 \alpha^{-3} \exp(-v^2/\alpha^2), \quad (1)$$

where α is the most probable velocity for the source oven temperature. The Ramsey lineshape computed from this velocity distribution agrees with the experimental lineshape within 1–2%. This implies a frequency uncertainty of $1\text{–}2 \times 10^{-14}$.

In the future, we plan to obtain velocity distributions from an inversion of Ramsey lineshapes recorded at different microwave powers. The inversion routine has a sensitivity to the quality of the input data that will produce an equivalent uncertainty of a few parts in 10^{15} per percent noise and a few parts in 10^{14} per decibel error in the microwave power ratios. This will allow the errors due to second-order Doppler shift to be reduced to no more than a few parts in 10^{15}.

Theoretical calculations show the second-order Doppler shift leads to a frequency sensitivity of about 10^{-14} per decibel change in microwave power at a power level about 3 dB below optimum. Near optimum the sensitivity is 2–3 times larger. There is also a sensitivity of 3×10^{-16} per percent change in modulation depth and 10^{-15} per degree change in phase of the demodulator reference signal. The stability of these parameters leads to an additional uncertainty of about 10^{-14} from the second-order Doppler shift.

IV. End-to-End Cavity Phase Shift

The end-to-end cavity phase shift has been measured by a beam reversal experiment. The frequency shift on beam reversal at optimum power was 1.52×10^{-12} with a 1 σ uncertainly of 3×10^{-14}. A numerical evaluation similar to that done for the second-order Doppler shift shows that this observed cavity phase shift corresponds to a phase difference between the two cavity ends of about 0.29 mrad. This is more than an order of magnitude larger than the phase difference anticipated from electrical measurements of cavity symmetry, which were made during fabrication. We now think this is due not to electrical asymmetry of the cavity, but rather to the overall dimension of the cavity, which allows a mode of odd symmetry to oscillate near the main cavity resonance [5].

The frequency correction for the cavity phase shift, about 7×10^{-13} in a given direction, is twice the second-order Doppler correction. But since the correction is proportional to v, whereas the second-order Doppler correction is proportional to v^2, its sensitivity to microwave power and modulation is similar to that of the second-order Doppler shift. Experimental measurements of power shift are in qualitative agreement with those expected theoretically for the combination of end-to-end cavity phase shift and second-order Doppler shift.

V. Other Cavity-Related Errors

The Q of the cavity is about 600. Cavity mistuning leads to a frequency bias which is less than 10^{-14} in the worst case and passes through zero near optimum power. Distributed-cavity phase errors are dramatically reduced in this standard by the use of cavity ends in which the Poynting vector approaches zero in the center of the atomic beam window [2] and by a very small atomic beam cross section (3 mm diameter). A search for distributed-cavity phase shift by alternatively blocking half of the atomic beam (in the direction of the waveguide) at one end of the cavity or the other showed no measurable effect at the 10^{-14} level.

VI. Line Overlap Shifts

Shifts from the overlap of other spectral lines [6], [7] have not yet been evaluated in detail. However, NIST-7 has three design features that greatly reduce such shifts. First, the microwave field amplitude in the direction of the atomic beam has a half-sine wave shape which greatly smooths and reduces the Rabi line wings relative to those in more conventional standards in which the field amplitude varies as a rectangular pulse. Second, the optical pumping is done with an orientation and polarization which produces no asymmetry in the Zeeman population distribution (see discussion in introduction). Finally, the optical pumping should result in equal velocity distributions in the various Zeeman levels. The top trace in Fig. 4 shows the high degree of spectral symmetry obtained. The asymmetry is less than 1% and corresponds to a shift of less than one part in 10^{15}. Transitions corresponding to $\Delta m_F = \pm 1$ are very small ($\leq 0.5\%$) and by all of the above arguments are very symmetric. Their contribution to line overlap shifts should be negligible.

VII. AC Stark Shifts

The shift due to blackbody radiation [8] can be calculated to very high accuracy since the temperature of the atomic beam tube of NIST-7 is regulated. For a $\Delta T = 0.1°C$, a shift of $\leq 10^{-16}$ is expected. The fluorescence light shift in NIST-7 is expected to be $\leq 10^{-16}$ [9]. Using different optical power levels and atomic beam flux, we have observed no frequency shifts at the 10^{-14} level.

VIII. Electronic Offsets

The present frequency control servo uses sine-wave phase modulation, square-wave demodulation, and a second-order loop filter. The modulator has second-harmonic distortion of less than -120 dBc [10]. The microwave radiation is synthesized by direct multiplication from the local oscillator at 5.006 880 MHz. The multiplier is characterized by a phase noise $\mathcal{L}(1 \text{ Hz}) = -140$ dBc, a noise floor $S_\phi \leq -170$ dBc, 5 MHz sidebands < -40 dBc, and sidebands from the power mains < -55 dBc. Unbalanced sidebands or single sidebands can not be generated by pure FM or PM but require an admixture of AM. Hence, use of a crystal detector and an FFT is a sensitive way to search for close-in, unbalanced sidebands. By using this technique, the unbalanced sidebands from the power mains have been shown to be ≤ -100 dBc. The spectral purity of the microwave radiation and

TABLE I
SUMMARY OF SYSTEMATIC ERRORS IN NIST-7. THE SIZE OF THE RESULTING BIAS IS GIVEN TOGETHER WITH THE ASSOCIATED UNCERTAINTY (ALL IN UNITS OF 10^{-14}). EXPERIMENTAL NUMBERS ARE COMPARED WITH MODEL ANALYSIS OF THE DESIGN OF THE STANDARD

Effect	Bias	Uncertainty (1σ)	
		Modeled	Measured
2nd-order Zeeman	$\approx 10{,}000$	0.3	1
2nd-order Doppler	≈ 30	0.3	2
Line overlap		0.1	—
AC Stark	1.9	0.1	1
Cavity phase	70	0.3	3
Electronics		0.3	1

the second-harmonic distortion in the modulator lead to errors $\leq 10^{-14}$.

To experimentally search for second-harmonic distortion in the modulator, the modulation depth was changed by a factor of 2. The search for DC offsets in the electronics, AC and DC gains were changed in such a way that the overall loop gain remained fixed. Gain changes of 2^7 were made. No frequency shifts were observed at the 10^{-14} level.

IX. SUMMARY

Limited analysis of frequency biasing errors in the NIST optically-pumped, primary frequency standard has been made. At present, all studied sources of error have been shown to be controllable to $\leq 3 \times 10^{-14}$ (see Table I) and suggest an overall accuracy of 4×10^{-14} (1σ). A more complete analysis of systematic effects with higher resolution measurements than those presented here is planned (and is necessary) to meet the full design accuracy of the standard. However, the device will functionally replace NBS-6 as our operational frequency standard in the very near future. Further developments in the servo electronics and laser systems are necessary before the standard can be operated as a *clock* at its full design potential.

ACKNOWLEDGMENTS

The authors would like to thank Dr. Fred Walls and Prof. Andrea DeMarchi for their numerous and invaluable contributions throughout this work.

REFERENCES

[1] Robert E. Drullinger, David J. Glaze, J. P. Lowe, and Jon H. Shirley, "The NIST optically pumped cesium frequency standard," *IEEE Trans. Instrum. Meas.*, vol. 40, pp. 162-164, Apr. 1991.
[2] A. DeMarchi, J. Shirley, D. J. Glaze, and R. Drullinger, "A new cavity configuration for cesium beam primary frequency standards," *IEEE Trans. Instrum. Meas.*, vol. 37, pp. 185-190, June 1988.
[3] G. Théobald, N. Dimarcq. V. Giordano, and P. Cérez, "Ground state Zeeman coherence effects in an optically pumped cesium beam," *Optics Comm.*, vol. 71, no. 5, pp. 256-262, June 1989.
[4] Jacques Vanier and Claude Audoin, *The Quantum Physics of Atomic Frequency Standards*. Bristol: U.K. IOP Publishing Ltd., 1989, chap. 5, pp. 785-791.
[5] A. DeMarchi, O. Francescangeli, and G. P. Bava, "Dimensional sensitivity of end-to-end phase difference in ring terminated Ramsey cavities," *IEEE Trans. Instrum. Meas.*, vol. 42, Apr. 1992.
[6] A. DeMarchi, G. D. Rovera, and A. Premoli, "Pulling by neighboring transitions and its effects on the performance of cesium-beam frequency standards,," *Metrologia*, vol. 20, pp. 37-47, 1984.
[7] L. S. Cutler, C. A. Flory, R. P. Giffard, and A. DeMarchi, "Frequency pulling by hyperfine σ transitions in cesium beam atomic frequency standards," *J. Appl. Phys.*, vol. 69, pp. 2780-2792, Mar. 1991.
[8] Wayne M. Itano, L. L. Lewis, and D. J. Wineland, "Shift of $^2S_{1/2}$ hyperfine splittings due to blackbody radiation," *Phys. Rev. A*, vol. 25, pp. 1233-1235, Feb. 1982.
[9] Jon Shirley, "Fluorescent light shift in optically pumped cesium standards," in Proc. 39th Freq. Cont. Symp., 1985, pp. 22-23.
[10] J. Lowe and F. Walls, "Ultralinear small-angle phase modulator," in Proc. 5th European Frequency and Time Forum, 1991, pp. 461-464.